Summer 8-2011

A Comparison of Two Different Methods for Solving Biharmonic Boundary Valve Problems

Megan LaShea Richardson
University of Southern Mississippi

The University of Southern Mississippi

A COMPARISON OF TWO DIFFERENT METHODS FOR SOLVING BIHARMONIC BOUNDARY VALUE PROBLEMS

by

Megan LaShea Richardson

A Thesis
Submitted to the Graduate School
of The University of Southern Mississippi
in Partial Fulfillment of the Requirements
for the Degree of Master of Science

Approved:

_Haiyan Tian_____
Director

_Joseph Kolibal_____

_C.S. Chen_____

_Susan A. Siltanen_____
Dean of the Graduate School

August 2011

ABSTRACT

A COMPARISON OF TWO DIFFERENT METHODS
FOR SOLVING BIHARMONIC BOUNDARY VALUE PROBLEMS

by Megan LaShea Richardson

August 2011

We use the methods of compactly supported radial basis functions (CS-RBFs) and Delta-shaped basis functions (DBFs) to obtain the numerical solution of a two-dimensional biharmonic boundary value problem. The biharmonic equation is difficult to solve due to its existing fourth order derivatives, besides it requires more than one boundary conditions on the same part of the boundary. In this thesis, we use either a one-level or a two-level technique for constructing the approximate solution in the context of Kansa's collocation method. This thesis will compare the accuracy of the methods of CS-RBFs and DBFs when applied to the biharmonic boundary value problem. Both methods can be used on an irregular shaped domain. Numerical results show that the DBF approach is superior than that of the CS-RBF.

ACKNOWLEDGMENTS

This is to thank all of those who have assisted me in this effort. This thesis would not have been possible without the time, patience, and guidance of my adviser, Dr. Haiyan Tian. In addition, I would like to thank Dr. Joseph Kolibal and Dr. C.S. Chen for serving on my committee and for their suggestions and guidance during the course of my research. I would also like thank my fellow colleagues for their suggestions and support. Last, but definitely not least, I would like to thank my family and friends for their continuous love, support, and encouragement.

TABLE OF CONTENTS

ABSTRACT ii

ACKNOWLEDGMENTS iii

LIST OF ILLUSTRATIONS v

LIST OF TABLES vi

NOTATION AND GLOSSARY vii

1 INTRODUCTION **1**

2 TWO DIFFERENT BASIS FUNCTIONS **4**
2.1 Compactly Supported Radial Basis Function 4
2.2 Delta-Shaped Basis Functions 5

3 COMPARISON OF BASIS FUNCTIONS **8**
3.1 Approximation of Solutions of PDEs 8
3.2 Numerical Results for a Second-Order PDE 9
3.3 Solving Biharmonic Boundary Value Problems 12
3.4 Conclusion of the Comparison 18

4 CONCLUSION **19**

BIBLIOGRAPHY **20**

LIST OF ILLUSTRATIONS

Figure

3.1 The graph of the exact solution to the problem in Example 1. 11
3.2 The graph of the exact solution to the problem in Example 2. 13
3.3 The graph of the exact solution to the problem in Example 3. 14
3.4 The graph of the exact solution to the problem in Example 4. 16
3.5 The graph of the exact solution to the problem in Example 5. 17
3.6 The graph of (a) $I_{20,6}$ on [-1,1], and (b) $I_{20,6}$ on [0.25,1]. 18

LIST OF TABLES

Table

2.1 A List of Wendland's CS-RBFs 5

3.1 Example 1 by CS-RBFs $\varphi_{4,2}$ with $\alpha_1 = 0.473$, $\alpha_2 = 0.319$ 10
3.2 Example 1 by CS-RBFs $\varphi_{4,2}$ with $\alpha_1 = 1.0$, $\alpha_2 = 0.8$ 10
3.3 Example 1 by CS-RBFs $\varphi_{5,3}$ with $\alpha_1 = 1.0$, $\alpha_2 = 0.8$ 11
3.4 Example 1 by DBFs: $I_{10,4}$ and $I_{20,6}$ 11
3.5 Example 2 by CS-RBFs $\varphi_{4,2}$ with $\alpha_1 = 0.473$, $\alpha_2 = 0.319$ 12
3.6 Example 2 by DBFs $I_{10,4}$ and $I_{20,6}$ 13
3.7 Example 3 by CS-RBFs $\varphi_{4,2}$ with $\alpha_1 = 0.473$, $\alpha_2 = 0.319$ 14
3.8 Example 3 by DBFs $I_{10,4}$ and $I_{20,6}$ 14
3.9 Example 4 by CS-RBFs $\varphi_{4,2}$ with $\alpha_1 = 0.473$, $\alpha_2 = 0.319$ 15
3.10 Example 4 by DBFs $I_{10,4}$ and $I_{20,6}$ 15
3.11 Example 5 by CS-RBFs $\varphi_{4,2}$ with $\alpha_1 = 0.473$, $\alpha_2 = 0.319$ 17
3.12 Example 5 by DBFs $I_{10,4}$ and $I_{20,6}$ 17

NOTATION AND GLOSSARY

General Usage and Terminology

The notation used in this text represents fairly standard mathematical and computational usage. In many cases these fields tend to use different preferred notation to indicate the same concept, and these have been reconciled to the extent possible, given the interdisciplinary nature of the material. In particular, the notation for partial derivatives varies extensively, and the notation used is chosen for stylistic convenience based on the application. While it would be convenient to utilize a standard nomenclature for this important symbol, the many alternatives currently in the published literature will continue to be utilized.

The blackboard fonts are used to denote standard sets of numbers: $\mathbb{R}$ for the field of real numbers. The capital letters, $A, B, \cdots$ are used to denote matrices, including capital greek letters, e.g., Φ for a positive definite matrix. Functions which are denoted in boldface type typically represent vector valued functions, and real valued functions usually are set in lower case roman or greek letters. Lower case letters such as i, j, k, l, m, n and sometimes p and d are used to denote indices.

Vectors are typeset in square brackets, e.g., $[\cdot]$, and matrices are typeset in parentheses, e.g., $(\cdot)$. In general the norms are typeset using double pairs of lines, e.g., $||\cdot||$, and the absolute value of numbers is denoted using a single pairs of lines, e.g., $|\cdot|$.

Chapter 1

INTRODUCTION

The biharmonic equation is a fourth-order, linear partial differential equation that occurs naturally in a number of science and engineering fields [8, 22]. It is used in numerous real applications such as flexure of elastic plates, flow of particulate suspensions, flow of molten metals,and in the modeling of bio-fluid dynamics [4]. The biharmonic equation is difficult to solve due to the existing fourth order derivatives. Besides it is different from a second-order PDE in that more than one boundary conditions must be required on the same part of the boundary.

The term biharmonic is significant due to the fact that the function that it is describing satisfies the Laplace equation, or harmonic equation, twice explicitly [13]. Although the exact date that the biharmonic problem was introduced to mathematics is unknown, it is evident that it was introduced after the harmonic function since every harmonic function satisfies Laplace's equation is also biharmonic; the converse is not necessarily true [4, 13].

As an example of the biharmonic equation occurring in structural and continuum mechanics with applications to thin plates and beams [7], the equation

$$\nabla^4 u = \frac{K}{D},$$

models the transverse deflection of a thin plate with K being the uniform load per unit area and D being the bending rigidity. The biharmonic equation applied to thin plates and beams can have clamped or simply supported boundary conditions [7]. The boundary conditions of a clamped plate can be expressed as

$$\begin{aligned} u &= 0, \\ \frac{\partial u}{\partial n} &= 0, \end{aligned}$$

whereas a plate with simply supported boundary conditions can be expressed as

$$\begin{aligned} u &= 0, \\ \nabla^2 u &= 0. \end{aligned}$$

Let

$$L[u] = \nabla^4 u(x,y) = \frac{\partial^4 u}{\partial x^4} + \frac{\partial^4 u}{\partial y^4} + 2\frac{\partial^4 u}{\partial x^2 y^2}, \tag{1.1}$$

then we study the inhomogeneous biharmonic equation

$$L[u] = h(x,y), \quad (x,y) \in \Omega, \tag{1.2}$$

with the boundary conditions

$$u = f(x,y) \quad (x,y) \in \partial\Omega, \tag{1.3}$$

$$\frac{\partial u}{\partial n} = g(x,y) \quad (x,y) \in \partial\Omega, \tag{1.4}$$

where Ω is a simply connected domain in R^2 with a piecewise smooth boundary $\partial\Omega$, $\frac{\partial u}{\partial n}$ denotes the outward normal derivative of u on $\partial\Omega$, and f and g are the Dirichlet and Neumann data on $\partial\Omega$ respectively.

The Green's function $K(x,y;\xi,\eta)$ [10, 21] for the biharmonic equation with clamped plate boundary conditions is a solution of

$$\nabla^4 K(x,y;\xi,\eta) = -\delta(x-\xi)\delta(y-\eta),$$

that satisfies the boundary conditions $K(x,y;\xi,\eta)\mid_{\partial\Omega} = 0$ and $\partial K(x,y;\xi,\eta)/\partial n \mid_{\partial\Omega} = 0$ where δ is the Dirac delta function and (ξ,η) is the source point where a unit load is applied. On the basis of the identity $u\nabla^2\nabla^2 v - v\nabla^2\nabla^2 u = \nabla\cdot\mathbf{p}$, where $\mathbf{p} = u\nabla\nabla^2 v - v\nabla\nabla^2 u + (\nabla^2 u)\nabla v - \left(\nabla^2 v\right)\nabla u$, and the divergence theorem, we obtain Green's theorem for an arbitrary region Ω [21],

$$\iint_\Omega \left[u\nabla\nabla^2 v - v\nabla\nabla^2 u\right] dxdy = \int_{\partial\Omega} \left[u\frac{\partial\left(\nabla^2 v\right)}{\partial n} - \left(\nabla^2 v\right)\frac{\partial u}{\partial n} + \left(\nabla^2 u\right)\frac{\partial v}{\partial n} - v\frac{\partial\left(\nabla^2 u\right)}{\partial n}\right] ds.$$

If $u(x,y)$ satisfies the inhomogeneous biharmonic equation (1.2) in Ω and boundary conditions (1.3)–(1.4) on $\partial\Omega$, then the Green's theorem for an arbitrary region Ω with $v = K(x,y;\xi,\eta)$ yields

$$\begin{aligned} u(\xi,\eta) = & -\iint_\Omega K(x,y;\xi,\eta)h(x,y)dxdy \\ & + \int_{\partial\Omega}\left[\left(\nabla^2 K(x,y;\xi,\eta)\right)g(x,y) - f(x,y)\frac{\partial\left(\nabla^2 K(x,y;\xi,\eta)\right)}{\partial n}\right] ds. \end{aligned}$$

As a result of Green's theorem, we have a fairly complicated domain integral that can be extremely difficult to solve, especially for an irregular shaped domain Ω. Although it is possible to construct the Green's function for the case of a circular clamped plate using special techniques, in general, it is impossible to construct the Green's function for a domain of irregular shape.

To avoid using Green's function and calculating complicated domain integrals, we will use multi-level compactly supported radial basis function (CS-RBF) and multi-level Delta-shaped basis function (DBF) methods to obtain the numerical solution of the biharmonic boundary value problem (1.2)–(1.4). Both methods can avoid domain discretization using a mesh which can be very time consuming. I chose to compare CS-RBFs and DBFs because they share similar features in that DBFs are approximately compactly supported.

Chen *et al.* [2] used a multi-level approach of CS-RBFs for solving PDEs. Their approach is to use a larger support basis with a small number of interpolation points in the initial level, then apply the smaller support basis with a larger number of interpolation points on the approximation of the residue of the previous level. In our two-level technique, we use more basis functions of smaller support, which leads to a similar effect in solving PDEs.

We use these CS-RBFs and DBFs in the context of Kansa's collocation method to find an approximate solution of the two dimensional biharmonic boundary value problem. Instead of approximating the source term h, we approximate the solution of u of (1.2)–(1.4) directly; therefore, the intermediate step of finding a particular solution is not needed [14].

In Chapter 2, we give introduction to the CS-RBFs and DBFs. In Chapter 3, we compare the solution by these two basis functions when applied to a second order PDE. We also apply the two methods to the biharmonic boundary value problem (1.2)–(1.4). The numerical results show that the DBF approach is superior than that of the CS-RBF approach.

Chapter 2

TWO DIFFERENT BASIS FUNCTIONS

2.1 Compactly Supported Radial Basis Function

In this section, we give introduction to the compactly supported radial basis functions. The first CS-RBFs were constructed by Wu [19], and shortly thereafter by Wendland [16]. In recent years, they have become very popular in practical use due to their computational appeal [3, 9, 14, 20]. This paper focuses on the CS-RBFs constructed by Wendland.

The Wendland CS-RBFs are constructed using the operator I and the univariate function ϕ_l

$$I(f)(r) = \int_r^\infty t f(t) dt,$$

and

$$\phi_l(r) = (1-r)_+^l = \begin{cases} (1-r)^l, & if\, 0 \le r \le 1, \\ 0, & if\, r > 1. \end{cases}$$

Let $\Phi : \mathbb{R}^{\mathrm{d}} \to \mathbb{R}$ be a radial function $\Phi(x) = \phi(\|x\|)$ with a univariate function $\phi : \mathbb{R}_{\ge 0} \to \mathbb{R}$ and the Euclidean norm $\|\cdot\|$. Φ is positive definite if for all data sets $\{x_1, \ldots, x_N\} \subseteq \mathbb{R}^{\mathrm{d}}$ of pairwise distinct points the interpolation matrix

$$A = \left(\Phi\left(x_j - x_k\right)\right)_{1 \le j,k \le N}$$

is positive definite.

Definition 2.1.1. A continuous function $\phi : \mathbb{R}_{\ge 0} \to \mathbb{R}$ is said to be positive definite on $\mathbb{R}^{\mathrm{d}}$, $\phi \in PD_d$, if the induced function $\Phi(x) := \phi(\|x\|)$, $x \in \mathbb{R}^{\mathrm{d}}$, is positive definite [16, 17].

The Wendland CS-RBFs $\varphi_{l,k} = I^k \phi_l$, with $l > 0$ has support in $[0,1]$. For every dimension d and every k, l can be chosen as $l = \lfloor \frac{d}{2} \rfloor + k + 1$ to have a $\varphi_{l,k}$ that is not only positive definite in space dimension d but also possesses $2k$ continuous derivatives around zero and $2k + \lfloor \frac{d}{2} \rfloor$ continuous derivatives around 1. Additionally, $\varphi_{l,k}(r)$ is of minimal polynomial degree among all positive definite radial basis functions satisfying the previously stated properties.

The above definition guarantees that an interpolation problem will have a unique solution for all sets of pairwise distinct centers $\left\{x_j, f(x_j)\right\}_{j=1}^N$. The function $\varphi_{l,k}(r)$ is a Wendland

CS-RBF with differentiability $2k$ for some $l \in N$. Table 2.1 contains Wendland's CS-RBFs when $d = 1, 3,$ and 5 [16]. Since the optimal function for $d = 2n$ and $d = 2n+1$ are equivalent, the same functions can be used for $d = 2$ and $d = 3$.

Table 2.1: *A List of Wendland's CS-RBFs*

$d = 1$	$\varphi_{1,0}(r) = (1-r)_+$	C^0
	$\varphi_{2,1}(r) \doteq (1-r)_+^3 (3r+1)$	C^2
	$\varphi_{3,2}(r) \doteq (1-r)_+^5 \left(8r^2+5r+1\right)$	C^4
$d = 3$	$\varphi_{2,0}(r) = (1-r)_+^2$	C^0
	$\varphi_{3,1}(r) \doteq (1-r)_+^4 (4r+1)$	C^2
	$\varphi_{4,2}(r) \doteq (1-r)_+^6 \left(35r^2+18r+3\right)$	C^4
	$\varphi_{5,3}(r) \doteq (1-r)_+^8 \left(32r^3+25r^2+8r+1\right)$	C^6
$d = 5$	$\varphi_{3,0}(r) = (1-r)_+^3$	C^0
	$\varphi_{4,1}(r) \doteq (1-r)_+^5 (5r+1)$	C^2
	$\varphi_{5,2}(r) \doteq (1-r)_+^7 \left(16r^2+7r+1\right)$	C^4

The CS-RBFs can be scaled with a shape parameter α. In order to improve the performance of the interpolation by CS-RBFs, different shape parameters may be employed [14, 18]. The CS-RBF $\varphi_{l,k}(r)$ has support of radius 1; therefore, the basis function

$$\varphi_{l,k}\left(\frac{r}{\alpha}\right),$$

has a support of radius $\alpha > 0$.

2.2 Delta-Shaped Basis Functions

In this section, we give an introduction to the Delta-shaped basis functions (DBFs). These basis functions are approximately compactly supported, and they have shown excellent performances when used to reconstruct surfaces with scattered data in regular or irregular domains and to approximate solutions of PDEs [11, 12, 14, 15]. DBFs have the form of a truncated series $I_{M,\chi}(x,\xi) = \sum_{n=1}^{M} c_n(\xi)\psi_n(x)$ over an orthogonal system ψ_n.

For the sake of simplicity, we first construct the one dimensional Delta-shaped basis

defined in the interval $[-1,1]$:

$$I_{M,\chi}(x,\xi) = \sum_{n=1}^{M} r_n(M,\chi)\psi_n(\xi)\psi_n(x),$$

where $(\psi_n(x),\mu_n)$ is a solution of the following Sturm-Liouville problem on the interval $[-1,1]$,

$$\psi'' = -\mu\psi, \;\; \psi(-1) = \psi(1) = 0.$$

Hence, the eigenfunctions and eigenvalues are respectively

$$\psi_n(x) = \sin\left(\frac{n\pi(x+1)}{2}\right),$$

and

$$\mu_n = \frac{n\pi}{2}, n = 1,2,\ldots.$$

The solutions $\{\psi_n(x),\mu_n\}$ satisfy the following conditions:

- $0 < \mu_1 < \mu_2 < \ldots < \mu_n \to \infty$, and
- the eigenfunctions $\psi_n(x)$ form an orthogonal system on $[-1,1]$ with a scalar product,

$$\int_{-1}^{1} \psi_n(x)\psi_m(x)dx = \begin{cases} 1, & if\ n = m, \\ 0, & if\ n \neq m. \end{cases}$$

The $r_n(M,\chi)$ are known as regularizing coefficients where M and χ are the scaling and regularizing parameters respectively. Here we use Riesz regularization technique,

$$\begin{aligned} r_n(M,\chi) &= \left[1 - \left(\frac{\mu_n}{\mu_{M+1}}\right)^2\right]^{\chi}, \\ &= \left[1 - \left(\frac{n}{M+1}\right)^2\right]^{\chi}. \end{aligned}$$

Thus, the Delta-shaped basis can be written in the form,

$$\begin{aligned} I_{M,\chi}(\mathrm{x},\xi) &= \sum_{n=1}^{M}\left[1 - \left(\frac{n}{M+1}\right)^2\right]^{\chi}\psi_n(\xi)\psi_n(x), \\ &= \sum_{n=1}^{M} c_n(\xi)\psi_n(x), \end{aligned}$$

where $c_n(\xi) = r_n(M,\chi)\psi_n(\xi)$.

A 2-D DBF can be obtained by multiplying two of 1-D basis functions,

$$I_{M,\chi}(\mathbf{x},\boldsymbol{\xi}) = I_{M,\chi}(x,\xi)I_{M,\chi}(y,\eta),$$

where $\mathbf{x} = (x,y)$ and $\boldsymbol{\xi} = (\xi,\eta)$. Hence,

$$\begin{aligned} I_{M,\chi}(x,y;\xi,\eta) &= \left(\sum_{n=1}^{M} c_n(\xi)\,\psi_n(x)\right)\left(\sum_{m=1}^{M} c_m(\eta)\,\psi_m(y)\right), \\ &= \sum_{n=1}^{M}\sum_{m=1}^{M} c_n(\xi)\,c_m(\eta)\,\psi_n(x)\,\psi_m(y). \end{aligned}$$

Similarly, a multi-dimensional Delta-shaped basis function can be obtained as a product of one dimensional basis functions; therefore, an N-dimensional Delta-shaped basis function can be written in the form

$$I_{M,\chi}(\mathbf{x},\boldsymbol{\xi}) = \prod_{i=1}^{N} I_{M,\chi}(x_i,\xi_i).$$

In our calculations of the solutions of PDEs, we use the DBFs $I_{10,4}$, and $I_{20,6}$. The approximate radii of support for these DBFs are respectively 0.473 and 0.319 [14]. A larger M results in a smaller radius of support. For the purpose of comparing the CS-RBFs and the DBFs, we use CS-RBFs with shape parameter values $\alpha = 0.473$ and $\alpha = 0.319$.

Chapter 3

COMPARISON OF BASIS FUNCTIONS

3.1 Approximation of Solutions of PDEs

In this section, we use both CS-RBFs and DBFs in Kansa's collocation [5, 6, 8, 14, 15] method to solve the biharmonic problem (1.2)–(1.4). We let $\Phi_\alpha(\xi;\mathbf{x})$ denote either a CS-RBF or a DBF with its center being ξ and its scaling factors resulting in a support of radius of α. Let $\left\{\xi^{(j)}\right\}_{j=1}^{K}$ be a set of center points of a chosen basis functions. In a one level approach, we express the solution of the PDE as a linear combination of a chosen basis function

$$\tilde{u}(x) = \sum_{j=1}^{K} p_j \Phi_\alpha\left(\xi^{(j)};\mathbf{x}\right), \tag{3.1}$$

where p_j are unknown coefficients to be determined.

We choose N_i collocation points $\{(x_i,y_i)\}_{i=1}^{N_i}$ in Ω, N_d collocation points $\{(x_i,y_i)\}_{i=N_i+1}^{N_i+N_d}$ on $\partial\Omega$, and N_n collocation points $\{(x_i,y_i)\}_{i=N_i+N_d+1}^{N_i+N_d+N_n}$ on $\partial\Omega$. By substituting (3.1) into (1.2)–(1.4) and making the equations hold true at the corresponding collocation points, we have the following linear system

$$\sum_{j=1}^{K} p_j L\left[\Phi_\alpha\left(\xi^{(j)};\mathbf{x}_i\right)\right] = h(\mathbf{x}_i), \quad \text{for} \quad i = 1,2,\ldots,N_i,$$

$$\sum_{j=1}^{K} p_j \left[\Phi_\alpha\left(\xi^{(j)};\mathbf{x}_i\right)\right] = f(\mathbf{x}_i), \quad \text{for} \quad i = N_i+1,\ldots,N_i+N_d,$$

$$\sum_{j=1}^{N} p_j \frac{\partial u}{\partial n}\left[\Phi_\alpha\left(\xi^{(j)};\mathbf{x}_i\right)\right] = g(\mathbf{x}_i), \quad \text{for} \quad i = N_i+N_d+1,\ldots,N_i+N_d+N_n.$$

In a multi-level approach, we express the solution of the PDE as a linear combination of basis functions of various scaling factors α_s, $s = 1,2,\ldots,S$. Corresponding to each α_s, K_s center points $\xi^{(s,j)} \in \Omega$, $j = 1,2,\ldots,K_s$ are chosen [14]. We let

$$\tilde{u}(x) = \sum_{s=1}^{S}\sum_{j=1}^{K_s} p_j \Phi_{\alpha_s}\left(\xi^{(s,j)};\mathbf{x}\right), \tag{3.2}$$

where p_j are unknown coefficients to be determined. By satisfying (1.2)–(1.4) at the corresponding collocation points, we have

$$\sum_{s=1}^{S}\sum_{j=1}^{K_s} p_{s,j} L\left[\Phi_{\alpha_s}\left(\xi^{(s,j)};\mathbf{x}_i\right)\right] = h(\mathbf{x}_i), \quad \text{for} \quad i=1,2,3,\ldots,N_i, \tag{3.3}$$

$$\sum_{s=1}^{S}\sum_{j=1}^{K_s} p_{s,j} \left[\Phi_{\alpha_s}\left(\xi^{(s,j)};\mathbf{x}_i\right)\right] = f(\mathbf{x}_i), \quad \text{for} \quad i=N_i+1,\ldots,N_i+N_d, \tag{3.4}$$

$$\sum_{s=1}^{S}\sum_{j=1}^{N} p_{s,j} \frac{\partial u}{\partial n}\left[\Phi_{\alpha_s}\left(\xi^{(s,j)};\mathbf{x}_i\right)\right] = g(\mathbf{x}_i), \quad \text{for} \quad i=N_i+N_d+1,\ldots,N_i+N_d+N_n, \tag{3.5}$$

where L is the biharmonic operator defined in (1.1). When $S=1$ in (3.3)–(3.5), it is a one-level approach.

Let $N=N_i+N_d+N_n$ denote the total number of collocation points and $K=K_1+\ldots+K_S$ denote the total number of center points.

- When $N=K$, we have a square matrix.
- When $N>K$, we have an overdetermined system of equations, which can be solved by using the least squares method.

Tian, *et al.*, [15] suggest that the number of collocation points N be approximately twice as many as the number of centers K for the DBF approach.

3.2 Numerical Results for a Second-Order PDE

We will calculate the mean squared error for the approximate solution using the following formula:

$$E_{sq}=\sqrt{\frac{1}{N_t}\sum_{t=1}^{N_t}\left[u(x_t,y_t)-\tilde{u}(x_t,y_t)\right]^2},$$

where u is the exact solution, $\tilde{u}$ is the approximate solution, and N_t is the total number of randomly distributed test points. We let $N_t=200$.

Example 1. We consider the modified Helmoltz equation defined on the square domain $\Omega=[-0.5,0.5]^2$ with Dirichlet boundary condition,

$$\begin{aligned} \triangle u(x,y)-10u(x,y) &= f(x,y),\ (x,y)\in\Omega, \\ u(x,y) &= g(x,y),\ (x,y)\in\partial\Omega. \end{aligned}$$

By letting $L = \Delta - 10$ in (3.3), we get a collocation system (3.3)–(3.4). When $S = 1$, it is a one-level method. When $S = 2$, it is a two-level method. Let $f(x,y)$ and $g(x,y)$ be given such that the exact solution is

$$u(x,y) = \sin\left(\frac{\pi}{6}(x+0.5)\right)\sin\left(\frac{7\pi}{4}(x+0.5)\right)\sin\left(\frac{3\pi}{4}(y+0.5)\right)\sin\left(\frac{5\pi}{4}(y+0.5)\right),$$

which is an oscillative, smooth surface shown in Figure 3.1. Randomly distributed points are used as the centers of the basis functions and collocation points inside Ω. The total number of collocation points on the boundary is 100. The numerical results by CS-RBFs and DBFs in one-level and two-level approaches are provided in Tables 3.1–3.4. Comparing the results in Tables 3.1 and 3.4, we notice that the DBF method has much better accuracy than CS-RBF. Also comparing Tables 3.1 and 3.2, we notice the accuracy of $\varphi_{4,2}$ CS-RBFs is improved when the scaling factors are larger. Now, comparing the results of CS-RBFs $\varphi_{4,2}$ in Table 3.2 with $\varphi_{5,3}$ in Table 3.3, we notice slight improvements in the accuracy due to the increased order of smoothness in the basis functions. Both the DBFs and CS-RBFs attain better accuracy when using a two-level approach.

Table 3.1: *Example 1 is solved by one-level and two-level CS-RBFs* $\varphi_{4,2}$ *with* $\alpha_1 = 0.473$, $\alpha_2 = 0.319$.

K	200	300	400	500
E by $\varphi_{4,2}$, $\alpha = 0.473$	1.5E-01	1.1E-01	1.3E-01	1.2E-01
E by $\varphi_{4,2}$, $\alpha = 0.319$	2.3E-01	2.4E-01	1.5E-01	1.4E-01
(K_1, K_2)	(50,150)	(100,200)	(100,300)	(100,400)
E by $\varphi_{4,2}$, $\alpha_1 = 0.473$, $\alpha_2 = 0.319$	1.6E-01	1.7E-01	1.3E-01	1.3E-01

Table 3.2: *Example 1 is solved by one-level and two-level CS-RBFs* $\varphi_{4,2}$ *with* $\alpha_1 = 1.0$, $\alpha_2 = 0.8$.

K	200	300	400	500
E by $\varphi_{4,2}$, $\alpha = 1.0$	9.46E-02	8.38E-02	9.23E-02	9.00E-02
E by $\varphi_{4,2}$, $\alpha = 0.8$	1.0E-01	8.85E-02	1.0E-01	9.65E-02
(K_1, K_2)	(50,150)	(100,200)	(100,300)	(100,400)
E by $\varphi_{4,2}$, $\alpha_1 = 1.0$, $\alpha_2 = 0.8$	8.95E-02	8.76E-02	9.01E-02	9.09E-02

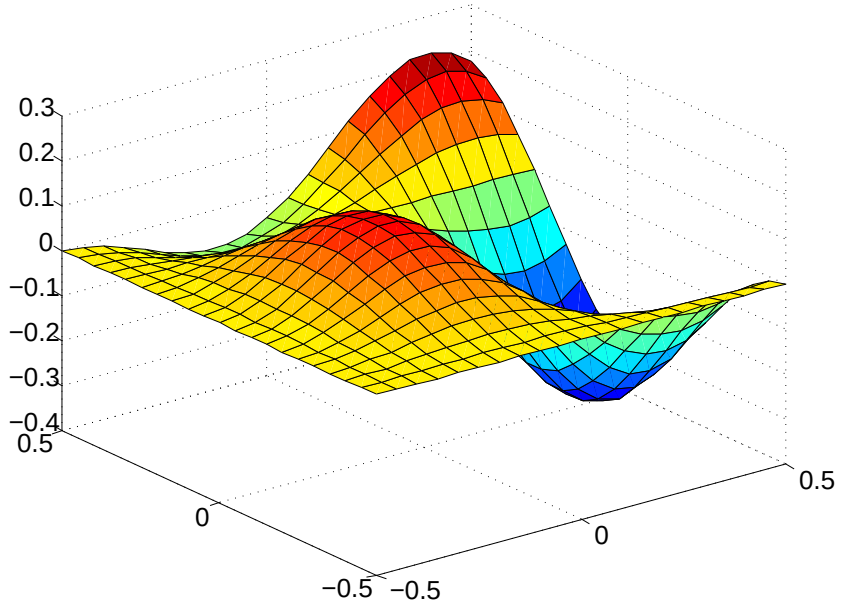

Figure 3.1: The graph of the exact solution to the problem in Example 1.

Table 3.3: *Example 1 is solved by one-level and two-level CS-RBFs* $\varphi_{5,3}$ *with* $\alpha_1 = 1.0$, $\alpha_2 = 0.8$.

K	200	300	400	500
E by $\varphi_{5,3}$, $\alpha = 1.0$	1.0E-01	3.14E-02	4.57E-02	4.51E-02
E by $\varphi_{5,3}$, $\alpha = 0.8$	8.67E-02	4.86E-02	5.38E-02	6.49E-02
(K_1, K_2)	(50,150)	(100,200)	(100,300)	(100,400)
E by $\varphi_{5,3}$, $\alpha_1 = 1.0$, $\alpha_2 = 0.8$	3.07E-02	1.10E-02	2.75E-03	2.40E-03

Table 3.4: *Example 1 is solved by one-level and two-level DBFs* $I_{10,4}$ *and* $I_{20,6}$.

K	200	300	400	500
E by $I_{10,4}$	1.3E-02	2.8E-02	4.2E-02	5.8E-02
E by $I_{20,6}$	5.1E-03	4.4E-05	5.5E-06	4.7E-06
(K_1, K_2)	(50,150)	(100,200)	(100,300)	(100,400)
E by $I_{10,4}$ & $I_{20,6}$	1.2E-03	2.9E-06	6.4E-06	5.2E-06

3.3 Solving Biharmonic Boundary Value Problems

In this section, we compare the error estimate of the Delta-shaped basis functions with the compactly supported radial basis functions applied to the biharmonic collocation system (3.3)–(3.5). Randomly distributed points are used as centers of the basis functions and the number of collocation points is twice the center points and the total number of boundary points is 100.

Example 2. We consider the biharmonic equation defined on the circular domain $x^2 + y^2 < \frac{1}{4}$ with the source function h, and the Dirichlet and Neumann data being respectively,

$$h(x,y) = 0,$$

$$f(x,y) = \frac{-\left(x^2+y^2\right)^2}{4},$$

$$g(x,y) = -\frac{b\left(\frac{x}{a}\right)\left(x^3+xy^2\right)}{\sqrt{a^2\left(\frac{y}{b}\right)^2+b^2\left(\frac{x}{a}\right)^2}} - \frac{a\left(\frac{y}{b}\right)\left(y^3+x^2y\right)}{\sqrt{a^2\left(\frac{y}{b}\right)^2+b^2\left(\frac{x}{a}\right)^2}},$$

where $a = 0.5$ and $b = 0.41665$. The exact solution is

$$u(x,y) = \frac{-\left(x^2+y^2\right)^2}{4},$$

which is an oscillative, smooth surface shown in Figure 3.2. This example is a homogeneous biharmonic boundary value problem. The numerical results by CS-RBFs and DBFs are provided in Tables 3.5 and 3.6. Comparing the results in Tables 3.5 and 3.6, we notice that the DBFs have slightly better accuracy than CS-RBFs.

Table 3.5: *Example 2 is solved by one-level and two-level CS-RBFs* $\varphi_{4,2}$ *with* $\alpha_1 = 0.473$, $\alpha_2 = 0.319$.

K	200	400
E by $\varphi_{4,2}$, $\alpha = 0.473$	9.7E-04	9.76E-04
E by $\varphi_{4,2}$, $\alpha = 0.319$	9.7E-04	9.76E-04
(K_1, K_2)	(50,150)	(100,300)
E by $\varphi_{4,2}$, $\alpha_1 = 0.473$, $\alpha_2 = 0.319$	9.7E-04	9.76E-04

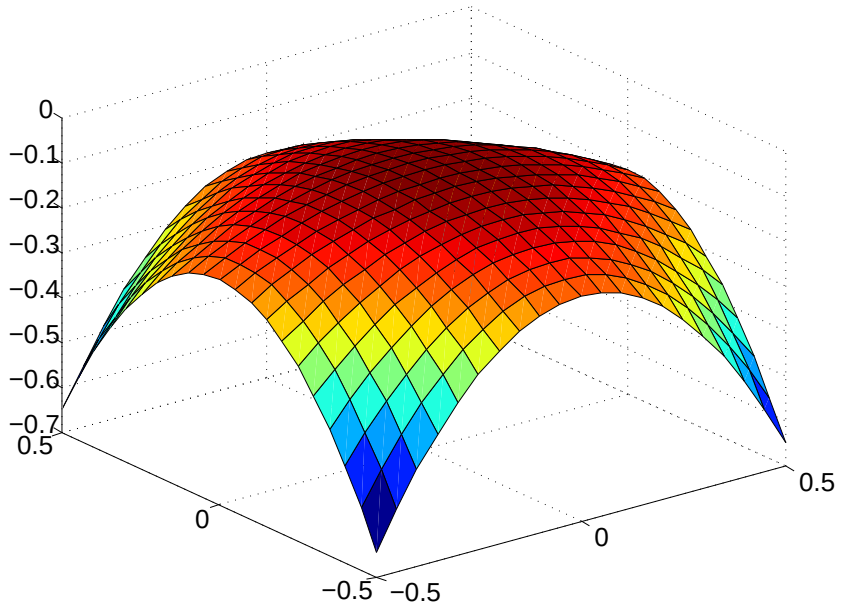

Figure 3.2: The graph of the exact solution to the problem in Example 2.

Table 3.6: *Example 2 is solved by one-level and two-level DBFs* $I_{10,4}$ *and* $I_{20,6}$.

K	200	300	400
E by $I_{10,4}$	9.4E-04	9.2E-04	9.3E-04
E by $I_{20,6}$	9.4E-04	9.3E-04	9.3E-04
(K_1, K_2)	(50,150)	(100,200)	(100,300)
E by $I_{10,4}$ & $I_{20,6}$	9.4E-04	9.2E-04	9.8E-04

Example 3. Consider the non-homogeneous biharmonic problem defined on the circular domain $x^2+y^2 < \frac{1}{4}$ with the source function h, and the Dirichlet and Neumann data being respectively,

$$h(x,y) = e^x,$$

$$f(x,y) = x^2+y^2+e^x,$$

and

$$g(x,y) = 8x^2+4xe^x+8y^2.$$

Its exact solution is

$$u(x,y) = x^2+y^2+e^x,$$

which is plotted in Figure 3.3. The numerical results by CS-RBFs and DBFs are provided in

Tables 3.7 and 3.8. Comparing the results in Tables 3.7 and 3.8, we notice the DBFs have better accuracy than CS-RBFs. Also, the accuracy of the DBFs is much better when it is increased from a one-level approach to a two-level approach.

Table 3.7: *Example 3 is solved by one-level and two-level CS-RBFs* $\varphi_{4,2}$ *with* $\alpha_1 = 0.473$, $\alpha_2 = 0.319$.

K	200	400
E by $\varphi_{4,2}$, $\alpha = 0.473$	1.3	1.3
E by $\varphi_{4,2}$, $\alpha = 0.319$	1.3	1.3
(K_1, K_2)	(50,150)	(100,300)
E by $\varphi_{4,2}$, $\alpha_1 = 0.473$, $\alpha_2 = 0.319$	1.3	1.3

Table 3.8: *Example 3 is solved by one-level and two-level DBFs* $I_{10,4}$ *and* $I_{20,6}$.

K	200	400
E by $I_{10,4}$	3.1E-03	1.7E-03
E by $I_{20,6}$	1.4E-02	1.0E-03
(K_1, K_2)	(50,150)	(150,250)
E by $I_{10,4}$ & $I_{20,6}$	2.3E-05	1.7E-06

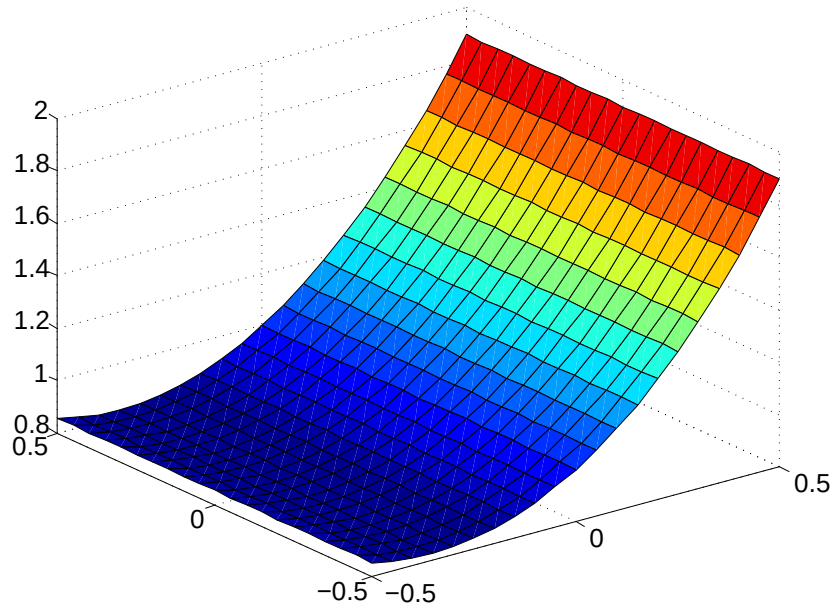

Figure 3.3: The graph of the exact solution to the problem in Example 3.

Example 4. We consider the non-homogeneous biharmonic problem defined on the circular domain $x^2+y^2<\frac{1}{4}$ with the source function,

$$h(x,y)=64\pi^4\cos(2\pi x+\pi)\cos(2\pi y+\pi)-16\pi^4\cos(2\pi x+\pi)-16\pi^4\cos(2\pi y+\pi),$$

and the Dirichlet and Neumann boundary data being respectively,

$$f(x,y)=(1-\cos(2\pi(x+0.5)))(1-\cos(2\pi(y+0.5))),$$

$$g(x,y)=(4x-4x\cos(2\pi(x+0.5)))(4y-4y\cos(2\pi(y+0.5))).$$

Its exact solution is

$$u(x,y)=(1-\cos(2\pi(x+0.5)))(1-\cos(2\pi(y+0.5))),$$

which is plotted in Figure 3.4. The numerical results by CS-RBFs and DBFs are provided in Tables 3.9 and 3.10. Comparing the results in Tables 3.9 and 3.10, we notice the DBFs provide much better accuracy than CS-RBFs.

Table 3.9: *Example 4 is solved by one-level and two-level CS-RBFs* $\varphi_{4,2}$ *with* $\alpha_1=0.473$, $\alpha_2=0.319$.

K	200	400
E by $\varphi_{4,2}$, $\alpha=0.473$	4.2	3.8
E by $\varphi_{4,2}$, $\alpha=0.319$	4.0	4.0
(K_1,K_2)	(50,150)	(100,300)
E by $\varphi_{4,2}$, $\alpha_1=0.473$, $\alpha_2=0.319$	4.1	3.8

Table 3.10: *Example 4 is solved by one-level and two-level DBFs* $I_{10,4}$ *and* $I_{20,6}$.

K	200	400
E by $I_{10,4}$	3.2E-03	2.3E-03
E by $I_{20,6}$	3.9E-03	2.0E-03
(K_1,K_2)	(50,150)	(50,350)
E by $I_{10,4}$ & $I_{20,6}$	5.3E-05	6.3E-06

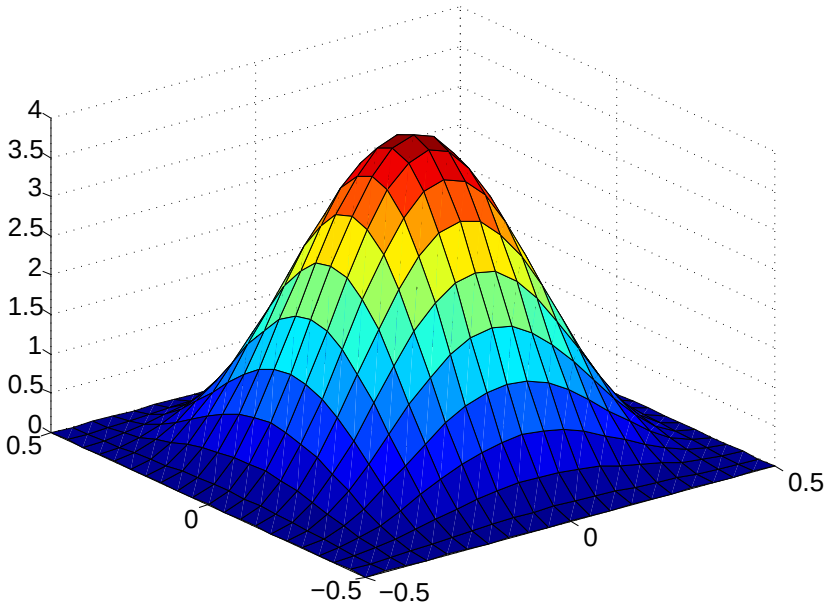

Figure 3.4: The graph of the exact solution to the problem in Example 4.

Example 5. In this example, we consider the non-homogeneous biharmonic problem defined on the circular domain $x^2+y^2<\frac{1}{5}$ with the source function,

$$\begin{aligned} h(x,y) &= -256\sin(4x)\sinh(4y)-512x\cos(4x)\sinh(4y)+512x\sin(4x)\cosh(4y) \\ &\quad -256\cos(4x)\cosh(4y), \end{aligned}$$

and Dirichlet and Neumann boundary data being respectively,

$$f(x,y)=2x\sin(4x)\cosh(4y)-2x\cos(4x)\sinh(4y),$$

$$\begin{aligned} g(x,y) &= 40x^2\sin(4x)\sinh(4y)-10x\cos(4x)\sinh(4y)+10x\sin(4x)\cosh(4y) \\ &\quad +40x^2\cos(4x)\cosh(4y)+40xy\sin(4x)\sinh(4y)-40xy\cos(4x)\cosh(4y). \end{aligned}$$

Its exact solution is

$$u(x,y)=2x\sin(4x)\cosh(4y)-2x\cos(4x)\sinh(4y),$$

which is an oscillative, smooth surface as shown in Figure 3.5. The numerical results by CS-RBFs and DBFs are provided in Tables 3.11 and 3.12. Comparing the results in Tables 3.11 and 3.12, we notice the DBFs have better accuracy than CS-RBFs. Although the DBFs have better accuracy than CS-RBFs, neither provide superior accuracy. The poor accuracy of both basis functions is due to the very limited number of collocation points chosen on the oscillating boundary Ω.

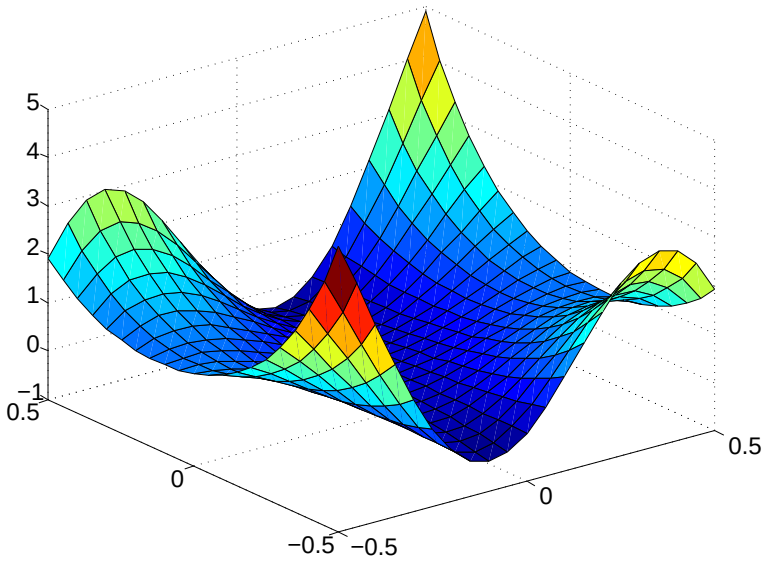

Figure 3.5: The graph of the exact solution to the problem in Example 5.

Table 3.11: *Example 5 is solved by one-level and two-level CS-RBFs* $\varphi_{4,2}$ *with* $\alpha_1 = 0.473$, $\alpha_2 = 0.319$.

K	200	400
E by $\varphi_{4,2}$, $\alpha = 0.473$	4.5E-01	5.0E-01
E by $\varphi_{4,2}$, $\alpha = 0.319$	4.6E-01	5.0E-01
(K_1, K_2)	(50,150)	(150,250)
E by $\varphi_{4,2}$, $\alpha_1 = 0.473$, $\alpha_2 = 0.319$	4.5E-01	5.0E-01

Table 3.12: *Example 5 is solved by one-level and two-level DBFs* $I_{10,4}$ *and* $I_{20,6}$.

K	200	400
E by $I_{10,4}$	7.6E-02	7.7E-02
E by $I_{20,6}$	7.7E-02	7.6E-02
(K_1, K_2)	(50,150)	(150,250)
E by $I_{10,4}$ & $I_{20,6}$	7.7E-02	7.6E-02

3.4 Conclusion of the Comparison

A CS-RBF is strictly zero outside its neighborhood of radius of support. A DBF appears to be zero outside of a neighborhood of ξ as shown in Figure 3.6 (a), but if we take a closer look at the same function on a smaller interval shown in Figure 3.6 (b) we can see that function values are not strictly zero outside of the neighborhood of ξ. Thus, DBFs are approximately compactly supported.

Despite the fact that the DBFs are approximately compactly supported, the excellent results obtained by the DBFs are due to the fact that they are globally supported and infinitely differentiable. The CS-RBF method can produce slightly better results when the scaling factors are increased and when the CS-RBF with higher smoothness are used. However, when we increase the scaling factors of the CS-RBF to 1.0 and 0.8 for the second-order PDE in Example 1, each basis function covers almost the entire domain. The resulting matrix is quite full, thus defeating the purpose of using the CS-RBFs. In such a case, the CS-RBF method is computationally inefficient, and it also produces poor results. Our numerical results show that the DBF method consistently produces better results.

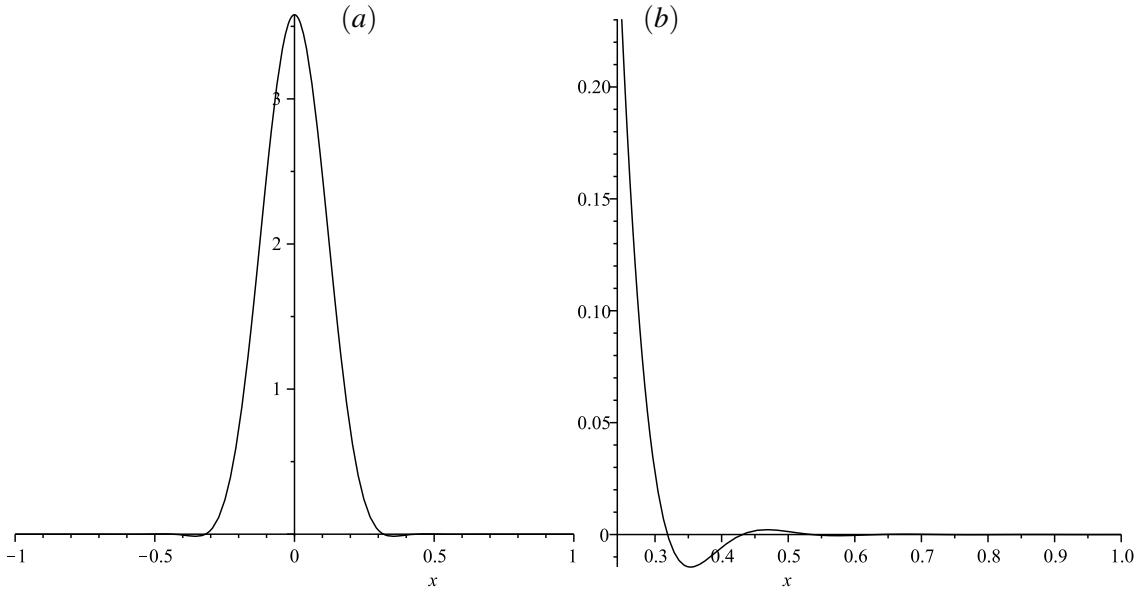

Figure 3.6: The graph of (a) $I_{20,6}$ on [-1,1], and (b) $I_{20,6}$ on [0.25,1].

Chapter 4

CONCLUSION

We compare the CS-RBFs with DBFs, which are approximately compactly supported, to obtain solutions of biharmonic boundary value problems. These methods help avoid domain discretization, thus they can effectively handle irregular shaped domains. In this thesis, both one-level and two-level techniques are used to solve the biharmonic boundary value problem. Due to the feature of the basis functions (compactly supported or approximately compactly supported), a two-level approach is used to improve the performance of the algorithm. From the numerical experiments we conducted, the method of Delta-shaped basis consistently produces more accurate solutions than that of the compactly supported basis. Since it is easy to construct multi-dimensional DBFs, the DBF method can be extended to solving multi-dimensional problems.

BIBLIOGRAPHY

[1] H. Adibi and J. Es'haghi. Numerical solution for biharmonic equations using multilevel radial basis functions and domain decomposition methods. *Applied Mathematics and Computation*, 186:246–255, 2007.

[2] C.S. Chen, M.A. Golberg, and R.A. Schaback. Recent developments of the dual reciprocity method using compactly supported radial basis functions. *Transformation of domain effects to the boundary*, pages 183–225, 2003.

[3] Michael S. Floater and Armin Iske. Multistep scattered data interpolation using compactly supported radial basis functions. *Journal of Computational and Applied Mathematics*, 73:65–78, 1996.

[4] J.P. Den Hartog. *Advanced strength of materials*. McGraw-Hill Inc., 1952.

[5] E.J. Kansa. Multiquadrics - a scattered data approximation scheme with applications to computational fluid-dynamics – I. surface approximations and partial derivatives estimates. *Computers and Mathematics with Applications*, 19:127–145, 1990.

[6] E.J. Kansa. Multiquadrics - a scattered data approximation scheme with applications to computational fluid-dynamics – II. solutions to parabolic, hyperbolic and elliptic partial differential equations. *Computers and Mathematics with Applications*, 19:127–145, 1990.

[7] Andreas Karageorghis and Graeme Fairweather. The method of fundamential solutions for the numerical solution of the biharmonic equation. *Journal of Computational Physics*, 69:434–459, 1987.

[8] J. Li. Application of radial basis meshless methods to direct and inverse biharmonic boundary value problems. *Communications in Numerical Methods in Engineering*, 21:169–182, 2005.

[9] Yi Lin and Ming Yuan. Convergence rates of compactly supported radial basis function regularization. *Statistica Sinica*, 16:425–439, 2006.

[10] George D. Manolis, Tsviatko V. Rangelov, and Richard P. Shaw. The non-homogeneous biharmonic plate equaiton: fundamental solutions. *International Journal of Solids and Structures*, 40:5753–5767, 2003.

[11] S. Reutskiy. A boundary method of trefftz type for pdes with scattered data. *Engineering Analysis with Boundary Elements*, 29:713–724, 2005.

[12] S. Reutskiy, C.S. Chen, and H.Y. Tian. A boundary meshless method using chebyshev interpolation and trigonometric basis function for solving heat conduction problems. *International Journal for Numerical Methods in Engineering*, 74:1621–1644, 2008.

[13] A.P.S. Selvadurai. *Partial Differential Equations in Mechanics*, volume 2. Springer, 2000.

[14] H.Y. Tian, H. Chi, and Y.Z. Cao. Comparing compactly supported radial basis with delta-shaped basis in solving elliptic problems. *International Journal of Computational Methods*, Preprint.

[15] H.Y. Tian, S. Reutskiy, and C.S. Chen. A basis function for approximation and the solutions of partial differential equations. *Numerical Methods for Partial Differential Equations*, 24(3):1018–1036, 2008.

[16] Holger Wendland. Piecewise polynomial, positive definite and compactly supported radial functions of minimal degree. *AICM*, 4:389–396, 1995.

[17] Holger Wendland. Error estimates for interpolation by compactly supported radial basis functions of minimal degree. *Journal of Approximation Theory*, 93:258–272, 1998.

[18] Jinming Wu and Renhong Wang. Approximate implicitization of parametric surfaces by using compactly supported radial basis functions. *Computers and Mathematics with Applications*, 56:3064–3069, 2008.

[19] Z.M. Wu. Multivariate compactly supported positive definite radial functions. *Advances in Computational Mathematics*, 4:283–292, 1995.

[20] J.R. Xiao. Local heaviside weighted mlpg meshless method for two-dimensional solids using compactly supported radial basis functions. *Computer methods in applied mechanics and engineering*, 193:117–138, 2004.

[21] Erich Zauderer. *Partial Differential Equations of Applied Mathematics*. Wiley, John & Sons, 2006.

[22] A. Zeb, L. Elliot, D.B. Ingham, and D. Lesnic. A comparison of different methods to solve inverse biharmonic boundary value problems. *International Journal for Numerical Methods in Engineering*, 45:1791–1806, 1999.